IEEE Access
Multidisciplinary | Rapid Review | Open Access Journal

Received 11 December 2023, accepted 21 December 2023, date of publication 1 January 2024,
date of current version 8 January 2024.

Digital Object Identifier 10.1109/ACCESS.2023.3348751

RESEARCH ARTICLE

A Fully Integrated Filtering Vivaldi Antenna With High Selectivity and Wide Out-of-Band Suppression

AHMAD EMADEDDIN AND B. L. G. JONSSON
KTH Royal Institute of Technology, 16261 Stockholm, Sweden

Corresponding author: Ahmad Emadeddin (ahmade@kth.se)

This work was supported in part by the Strategic Innovation Program Smarter Electronics System—A Joint Effort by Vinnova, Formas and Energimyndigheten (Energy Agency) under Project 2022-00833; and in part by the Swedish Foundation for Strategic Research under Project ID20-0004.

ABSTRACT This paper introduces a novel filtering approach that employs integrated periodic structures with a conventional Vivaldi antenna to achieve a fully integrated bandpass filtering antenna. The approach results in a wide out-of-band suppression, high passband selectivity, adjustable operational bandwidth, and low insertion loss. The proposed filtering approach maintains the original size of the conventional Vivaldi antenna (base antenna) without requiring additional modifications. To validate the approach, we present two filtering Vivaldi antennas: filtering antenna I (center frequency: 18GHz, fractional bandwidth: 21%, insertion loss: 0.32dB) and filtering antenna II (center frequency: 6.5GHz, fractional bandwidth: 12%, insertion loss: 0.6dB). Their wide out-of-band gain suppression (typically $\geq$15dB) covers the conventional Vivaldi antenna's frequency range (4-24GHz). A prototype of the filtering antenna I is manufactured. Its measurement results validate the proposed approach and show good agreement with the simulated reflection coefficient, realized gain, and radiation patterns. The features of the proposed filtering antenna approach, make it suitable for various applications requiring efficient frequency filtering.

INDEX TERMS Filtering antenna, fully integrated antenna design, metasurface, out-of-band suppression, wideband antenna, filtenna.

I. INTRODUCTION

wireless communication systems play a significant role in modern technology, such as mobile communication, satellite communication, and radars. Utilizing wideband antennas in such systems yields numerous benefits, such as versatility, simplification, cost, and space savings [1]. Besides, it is crucial to use specific filters in order to ensure the best performance of these systems. The filters provide a dual function by preventing the emission and/or receiving of signals outside the desired frequency range during transmission and reception. Moreover, enhancing wideband antennas with filtering functions allows for the flexible selection of desired bandwidth while maintaining consistent antenna behavior. This enhancement improves their adaptability across diverse scenarios and applications, e.g. 5G base stations, directional communication, radar systems, and passive sensors.

Traditionally, external filter modules, located at various points along the signal path, have been used to filter out-of-band emissions. However, the size and price of these traditional filters are typically significant drawbacks. This challenge becomes even more complicated in active antennas, where some of the filters should be placed between the antenna element and the integrated power amplifiers/LNAs in their corresponding transmitter and receiver chains. In this situation, there are two major challenges: Firstly, when the antenna element is highly integrated with transceiver components, there is significantly less space left for filtering. Secondly, in the highly integrated active antenna, the standard 50 Ω interface impedance can not be applied in the case of high-efficiency requirement [2], [3].

The associate editor coordinating the review of this manuscript and approving it for publication was Hassan Tariq Chattha.

An innovative idea known as antenna-integrated filters, filtering antennas, or filtenna has been presented to address these challenges [4]. By combining the functionality of antennas and filters into one structure, this idea reduces the need for separate, standard 50 Ω, and large-scale filter components. In the effort to develop these filtering antennas, a variety of approaches have been recently investigated in [4], [5], and [6].

Apart from the standard 50 Ω interface, the integration of the filtering antenna can be categorized into two integration levels: high integration and full integration. In high integration, 50 Ω interface impedance is eliminated and the filter is directly connected to the base antenna in an optimum interface impedance. However, compared to the base antenna, this method results in an increase in the filtering antenna's overall size. Good examples of the recent highly integrated filtering antenna have been presented in [7], [8], [9], [10], [11], [12], [13], [14], and [15]. On the other hand, full integration entails designing an integrated antenna that doesn't need either the 50 Ω interface impedance nor any increase in size to the base antenna. In [16], [17], [18], [19], [20], and [21], a number of novel instances of fully integrated filtering antennas have been reported. These include the incorporation of a narrow band-pass resonator on Vivaldi antenna [22], radiation null on a narrow band substrate integrated waveguide slot antenna [23] and on the metasurface antenna [24], the implementation of a notched-band on wideband Vivaldi antenna [25], and harmonic suppression on narrowband patch antenna [26]. However, it's worth mentioning that these filtering approaches have their specific areas of focus, such as creating a narrow passband, improving antenna bandwidth, integrating null, or suppressing harmonics (lowpass filters). This paper introduces a novel fully integrated band-pass filtering antenna based on a wideband Vivaldi antenna. Our focus is on the unique capabilities of passband selectivity and operational bandwidth tuning across the wide bandwidth of the base antenna.

Another desired characteristic of filtering antennas, especially in high-power systems, is wide out-of-band suppression. In [10], a low-pass filter has been highly integrated by a narrowband stepped-impedance dipole antenna to suppress the gain of upper harmonic ≥10dB up to 4.8×center frequency. In [27], a highly integrated filtering Vivaldi antenna utilizes slotline surface plasmon polaritons, reported in [28], to filter out the frequencies above 27GHz with out-of-band gain suppression of about 14dB. In [29], the band-pass filtering Vivaldi antenna array incorporates a low-pass filter, realized by periodically slotline's corrugation, and a high-pass filter realized by surrounding the antenna with a waveguide. Its fractional passband bandwidth is 88% (1.2-3.1GHz) with upper band gain suppression of ≥20dB up to 6GHz. The ability to control the lower edge frequency of the filtering antenna has not been addressed in [10] and [27] and the authors have used the lower cutoff antenna frequency. Moreover, in [29], due to incorporating a waveguide to control the lower edge frequency, the adjustment becomes complicated. Furthermore, operational bandwidth tuning has not been addressed in the literature.

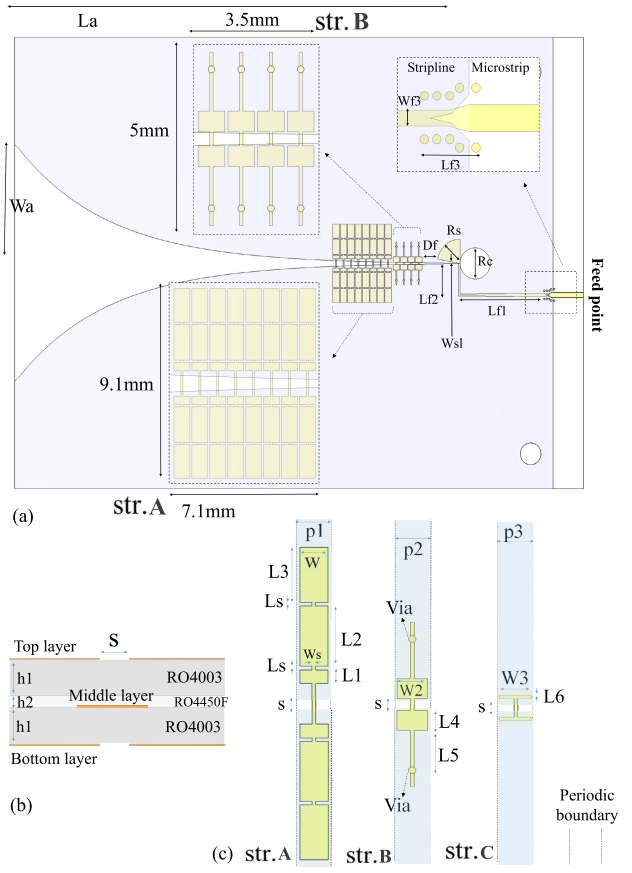

FIGURE 1. (a) Top view of the filtering Vivaldi antenna I operating from 15.6 to 19.3GHz, (b) side view, (c) proposed filtering periodic structures.

In this paper, we introduce a new approach involving novel periodic structures which are fully integrated into the conventional Vivaldi antenna. The design of our proposed multi-functional filtering antenna, filtenna, simultaneously incorporates four key features, representing a groundbreaking development in the field. This unique combination of functionalities within a geometry sets our work apart from existing literature. The key features are:

- the integration results in a fully integrated filtenna, that maintains its original dimensions without requiring any additional adjustments,
- the ability of passband selectivity within the broader frequency spectrum of the wideband Vivaldi antenna, without relying on the antenna's aperture cutoff frequencies at both lower and higher filtering frequency edges,
- the capability of adjusting the operational bandwidth (from very wide to narrow bandwidth, it can even function as a notch filter),
- low insertion loss with a wide out-of-band suppression range.

We demonstrate the approach by designing two filtering Vivaldi antenna prototypes, achieving low in-band insertion

TABLE 1. Dimensions of the proposed configurations (mm).

Parameter	Description	Value
Wa	half of the max. flare width	13
La	flare length	53
h1	substrate thickness	0.3
h2	PP thickness	0.1
Rc	cavity diameter	3.7
Rs	radial stub length	2.7
Wsl	minimum slotwidth	0.17
Lf1	1st length of feeding line	10
Lf2	2nd length of feeding line	3.8
Lf3	microstrip to stripline trans.	1.4
Wf3	stripline width	0.33
Df	distance B.W. feeding and filtering str. (filtenna I)	1.9
Df	distance B.W. feeding and filtering str. (filtenna II)	1.15
p1	str. A periodicity (filtenna I)	0.9
p2	str. B periodicity (filtenna I)	0.9
p2	str. A periodicity (filtenna II)	1
p3	str. C periodicity (filtenna II)	2.4
W	str. A width (filtenna I)	0.8
W2	str. B width (filtenna I)	0.8
W	str. A width (filtenna II)	0.9
W3	str. C width (filtenna II)	2.3
Ls	str. A stepped length (filtenna I and II)	0.1
Ws	str. A stepped width (filtenna I and II)	0.1
L1	str. A 1st length (filtenna I)	0.4
L2	str. A 2nd length (filtenna I)	1.75
L3	str. A 3rd length (filtenna I)	1.6
L1	str. A 1st length (filtenna II)	1.75
L2+L3	str. A 2nd+3rd length (filtenna II)	10.1
L4	str. B 4th length (filtenna I)	0.6
L5	str. B 5th length (filtenna I)	1.26
L6	str. C 6th length (filtenna II)	0.3

losses of 0.32 dB and 0.6 dB using an identical Vivaldi base antenna. These filtering antennas represent operational bandwidths of 21% at 18 GHz and 12% at 6.5 GHz, respectively. Moreover, the filtennas feature a wide out-of-band gain suppression of typically $\geq$15dB. In addition to the filtering bandwidth and center frequency, the out-of-band suppression level and range can also be adjusted according to the desired application.

II. DESIGN PRINCIPLE

In this section we first recall the traditional Vivaldi antenna, also referred to as the exponentially tapered slot antenna. Here we utilize it as the base antenna element. Subsequently, the novel filtering structures (referred to as str. A, B, and C) and their combinations are discussed in detail. The dispersion diagram results, reported in this section, are obtained utilizing CST Studio Suit eigenmode solver with a one-dimension periodic boundary condition.

A. VIVALDI ANTENNA

The need for antennas with characteristics like wide bandwidth and directional radiation patterns has grown along with the demand for wireless communication. One of the viable candidates for a broadband directional communication system is the Vivaldi antenna. This kind of antenna is thoroughly described in various literature, e.g. [1] and [30], and recently reviewed in [31]. In this paper, the Vivaldi

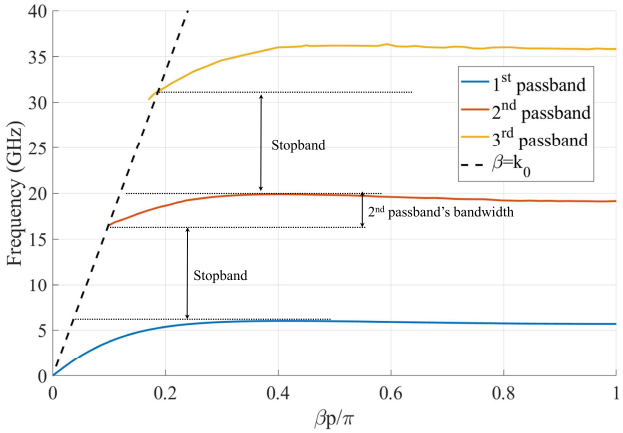

FIGURE 2. Dispersion diagram of the proposed structure A up to 40GHz with three distinct passbands and two stopbands (p1=0.9mm, W=0.8mm, L3=1.6 mm, Ws=0.1mm, and s=0.4mm). The second passband is the desired passband frequency range.

element, Fig. 1(a) and 1(b), is implemented on a 3-layer PCB technology, realizing stripline configuration. It consists of two Rogers RO4003C substrates (0.3mm thickness), a RO4450F as prepreg (0.1mm thickness), and 3-layer 1 oz copper cladding. The tapered slot patterns of the Vivaldi elements are placed on both the top and bottom sides of the structure. The feed line, along with the radial stub, is positioned on the middle layer. Here, a broadband microstrip to stripline transition, [32], is employed for easy connectorizing of the multilayer structure. The designed conventional Vivaldi antenna, simulated in CST Studio Suit transient solver, results in a below -10dB reflection coefficient across a frequency range of 4-24GHz and a maximum realized gain of 9.5dB. The dimensions of the base element are reported in Table 1.

The performance of the Vivaldi antenna can be enhanced by utilizing different previously reported techniques. These techniques include the incorporation of spoof surface plasmon polaritons (corrugation) along the flare or edge [27], [33], [34], sliced notch antenna [35], dielectric director and slab [36], [37], parasitic elements [8], and metamaterials [27], [38].

Although such techniques can be applied to our base antenna structure, they have not been incorporated in this paper. The present paper focuses on demonstrating the filtering performance of the proposed structures without any contribution from other techniques. This choice is made to enhance clarity and readability while showcasing the filtering structures' capabilities. Thus, we have kept the base antenna simple and have not used any of the advanced techniques mentioned.

B. FILTERING STRUCTURE A

The concept of loading a Vivaldi antenna by a short-circuited stepped impedance resonator to achieve a notched pole was introduced in [25]. Wherever the resonator represents a short

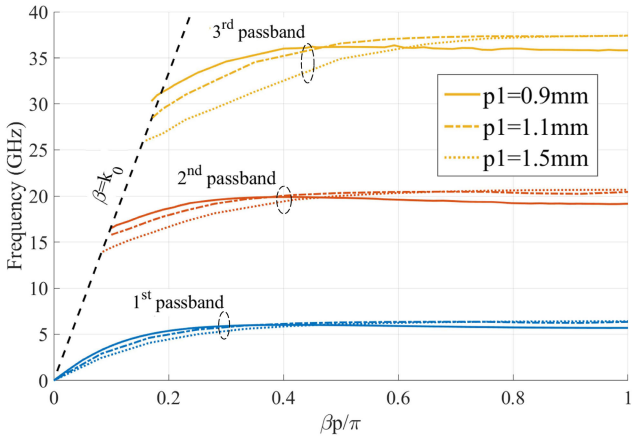

FIGURE 3. Dispersion diagram of the proposed structure A up to 40GHz with W=0.8mm, L3=1.6mm, Ws=0.1mm, s=0.4mm, and varying periodicity p1.

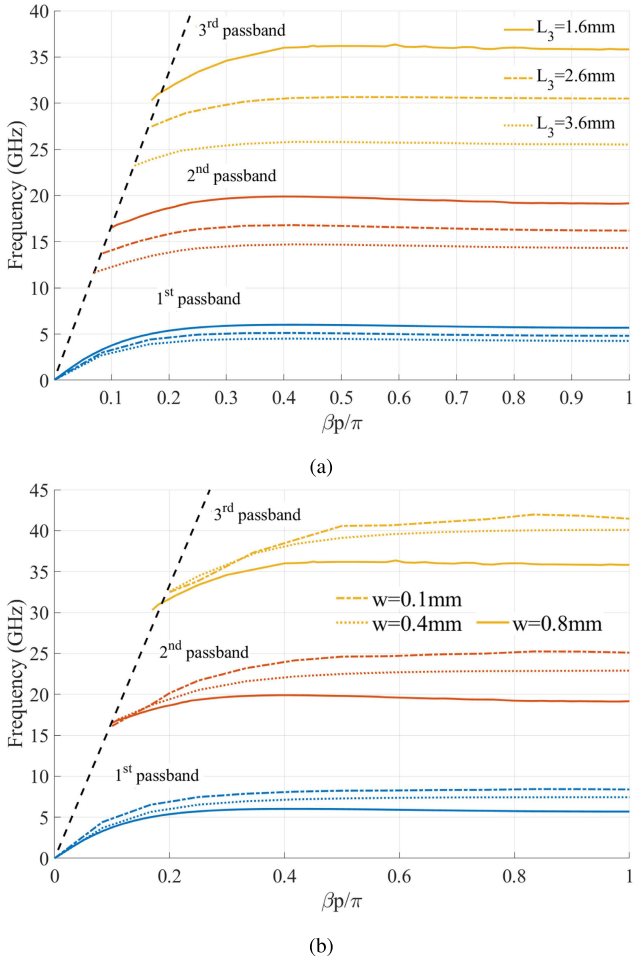

FIGURE 4. Dispersion diagram of the proposed structure A with (a) p1=0.9 mm, W=0.8mm, Ws=0.1mm, s=0.4mm, and varying patch length L3 for band selectivity, (b) p1=0.9mm, L3=1.6mm, Ws=0.1mm, s=0.4mm, and varying width W for operational bandwidth tuning.

circuit across the frequency spectrum, the intended notched pole is achieved. However, in pursuit of our paper's objective, which is a fully integrated band-pass filtering antenna with high selectivity, adjustable operational bandwidth, and wide out-of-band suppression, we develop a novel concept. This concept leverages the incorporation of the properties of periodic and guiding structures, as explored in prior research [39], to the idea of the notched pole. Through the incorporation of periodic-loaded lines and an understanding of their dispersive properties, we demonstrate that the frequency response of the structures is divided into distinct pass bands and stop bands. Utilizing these principles, we have effectively widened the stopband, compared to the notched pole, to cover a broader range of frequencies. Furthermore, we achieve an adjustable passband that is bordered by these stopband regions. This configuration provides control of the filtering performance according to desired specifications.

The first structure, referred to as str. A, is depicted in Fig. 1(c). It fulfills the necessary criteria of an adjustable passband with wide stopbands. All filtering structures are positioned in the middle layer. The parameter dimensions of the str. A are detailed in Table 1. The parameters such as periodicity p1, width W, patch length L3, and stepped width Ws act as effective controls for tuning the stop/pass band frequencies and the operational bandwidth. The dispersion characteristics of structure A are shown in Fig. 2, in which the 1st, 2nd, and 3rd passband frequencies are plotted for p1=0.9mm, W=0.8mm, L3=1.6mm, and Ws=0.1mm. It's worth noting that in this figure, the slotline width s is set to 0.4mm.

The initial passband begins at a very low frequency, which aligns with the expected capacitive behavior of the proposed periodic structure A —- representing an open circuit at lower frequencies. This passband extends to the cutoff frequency of 6GHz, Above that point, the first stopband extends to 16GHz. Subsequently, the second passband, which is the desired operating frequency range, appears between 16-20GHz exhibiting a fractional bandwidth of 22%. This is followed by another stopband that lasts until 31GHz. The propagation of electromagnetic energy across the slotline is essentially stopped within the stopband regions. The observed behavior is a result of the proposed structure's ability to generate virtual short-circuits between the two sides of the slotline transmission line, leading to the desired filtering performance. The stopband of the filtering response can be also widened by the structure's tapering since shorter structures work better at higher frequencies.

The viability of only using structure A is dependent on the demands of the particular application; especially if the out-of-band suppression range shown in Fig. 2 is enough. It's important to emphasize that this controllable filtering performance can be tailored to meet specific requirements. It can also be combined with other structurally similar periodic structures, as we will demonstrate in the next sections.

In order to provide conceptual validation and demonstrate the impact of periodicity on the filtering response, we present the dispersion diagram of the structure with different periodicity values in Fig. 3. It is observed that by increasing

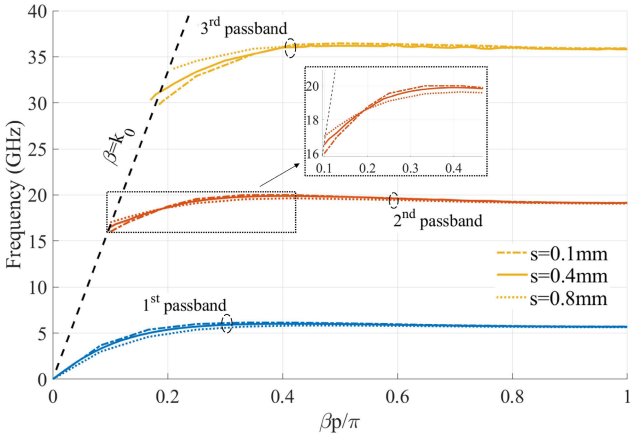

FIGURE 5. Dispersion diagram of the proposed structure A with p1=0.9mm, W=0.8mm, L3=1.6mm, Ws=0.1mm, and varying slotline's width s.

the periodicity, the stopbands become narrower, ultimately converging into a notched pole of a stepped impedance resonator. This emerges when the periodicity becomes large enough, leading to no interactions between the structure's units.

As pointed out before, to enhance the filtering performance of structure A in terms of out-of-band-suppression range, we will introduce other structurally similar configurations in the upcoming sections. However, we primarily analyze and elaborate on the performance of structure A to explain the filter's behavior. Given the structural similarity, our findings are applicable also to structures B and C, depicted in Fig. 1(c).

Recall that we are aiming for two key features at the filtenna: the ability of passband selectivity across the wide frequency range of the Vivaldi antenna and the capability of controlling the operational bandwidth. Thus, the proposed configuration should demonstrate the capabilities, exhibited in Fig. 4(a),4(b). Fig. 4(a) illustrates the band selectivity, or in other words adjusting the passband center frequency, while the fractional operating bandwidth is robust around 22% for the 2nd passband. Thus, tuning the length of the structure appears as a key parameter for achieving band selectivity, offering a straightforward method to adjust the filter's center frequency. Additionally, the concept of electronically tuning and shifting the passband–via the integration of PIN diodes to create distinct sections– can be incorporated into the configuration. However, consideration needs to be given to any potential parasitic effects across the different parts in the PIN diode scenario. Furthermore, it is observed that adjusting the width of the stepped-section Ws, Fig. 1(c), fine-tunes the passband center frequency by up to 10%.

Fig. 4(b) illustrates the impact of adjusting the width W that enables control over the operational bandwidth of the filtering performance. The upper cutoff frequencies of the passbands are affected by the width W, e.g. the 2nd passband's fractional bandwidth changes from 22% at W=0.8mm to 50% at W=0.1mm. Additionally, using periodicity, as shown in Fig. 3, allows for control of the operational bandwidth,

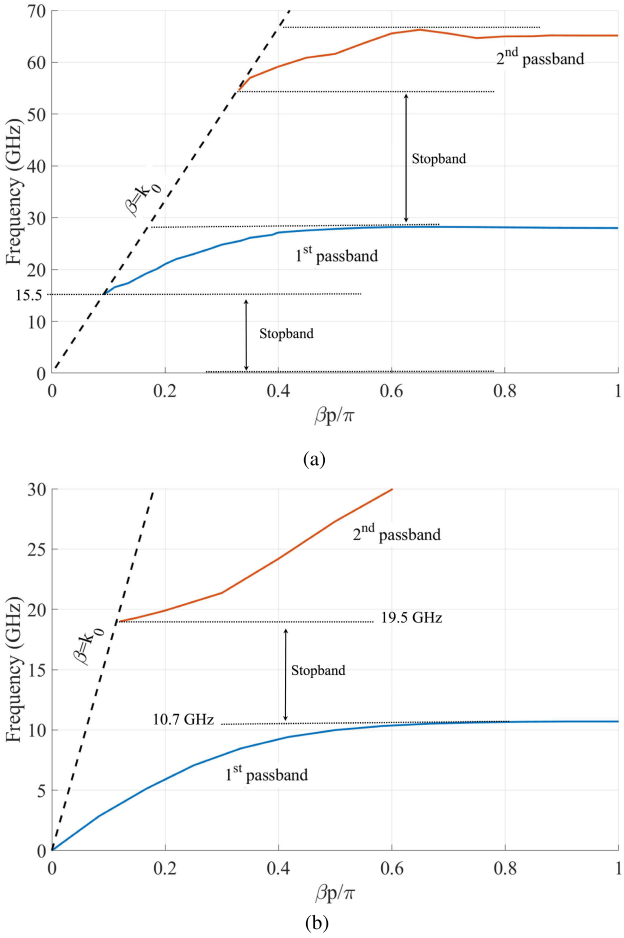

FIGURE 6. Dispersion diagram of the proposed (a) structure B with p2=0.9 mm, W2=0.8mm, L5=1.2mm, s=0.4mm, (b) structure C with p3=2.4mm, W3= 2.3mm, L6=0.3mm, s=0.4mm.

e.g. increasing periodicity widens the passband bandwidth, particularly at the lower cutoff frequency.

Given that the structure will be fully integrated into a Vivaldi antenna, where the slot line width varies within the antenna flare, it's essential to evaluate the effects of the variation of slotline's width on the filtering performance. Fig. 5 demonstrates that the variation in the slotline's width s has a negligible impact on the filtering performance. The enlarged view of the 2nd passband highlights the robustness. As a result, the filtering structures can be fully integrated along the antenna flare. Notably, according to the geometry of the structure, the presence of a strip parallel to the electric field vector below the slotline results in an increase in insertion loss if one moves very far along the flare where the slot width widens.

C. FILTERING STRUCTURE B AND C

As previously mentioned, utilizing solely structure A might be suitable for some applications. However, if a wider out-of-band suppression is needed, we here introduce two additional filtering configurations which have conceptual and structural similarities with structure A. Cascading of these structures together with str. A, results in a very wide suppression range.

Given the dispersion diagram of structure A, Fig. 2, cascading of another structure, featuring bandstop responses on both the 1st and 3rd passbands of structure A, effectively blocks their propagation. Hence, only the 2nd passband is permitted to propagate with a range starting from very low frequencies up to above 40GHz.

Through the incorporation of a short-circuited via on both sides of a conceptually and structurally similar geometry, depicted in Fig. 1(c)-structure B, any propagation at lower frequencies is blocked due to its inductive characteristics at those frequencies. Thus, the suppression of the 1st passband of structure A, Fig. 2, can be expected by tuning the cutoff frequencies of structure B. Recall that, given the structural similarity, all parameter analyses and findings presented in section II-B for structure A are also applicable to structures B and C, depicted in Fig. 1(c). Due to conciseness, we do not repeat the details for structures B and C. As a result, the starting frequencies and cutoff frequencies of the pass/stop bands are controllable for these structural similar configurations utilizing periodicity (p2 and p3), width (W2 and W3), and length (L4, L5, and L6).

Fig. 6(a) illustrates the dispersion diagram of structure B, which is tuned to align its second stopband with the 3rd passband of structure A, Fig. 2. Besides, it also aligns the upper cutoff frequency of the first stopband below 16GHz. In the case of cascading structures A and B, as depicted in Fig. 1(a), only a single passband (16-20GHz) remains, propagates, and radiates through the Vivaldi antenna.

In addition to structure B, we here introduce another conceptually and structurally similar configuration for cases requiring a passband at low frequency. This structure, named structure C and depicted in Fig. 1(c), can effectively work as a lowpass filter up to its next passband. This structure is similar to structure A but considerably smaller, designed to use its first passband as a lowpass filter. The dispersion diagram of structure C is exhibited in Fig. 6(b), where the stopband from 10.7GHz to 19.5GHz is adjusted utilizing the periodicity p3 and width W3, instead of its length L6. This approach was observed to provide a better impedance matching to the slotline in the first passband, starting from very low frequencies. On the other hand, using the length (e.g. L3 and L5) is recommended for structures A and B, to achieve a wider stopband. In our scenario, the Vivaldi antenna functions well from 4GHz up to 24GHz, inherently filtering out lower and higher frequencies.

As pointed out, these structures offer similar controllability as structure A but with a significantly wider passband. Solely employing one of the fully integrated structures can function as bandpass filters by leveraging the antenna aperture's cutoff frequencies, according to specific application requirements. The passband bandwidth can extend up to the entire bandwidth of the base antenna.

III. FILTERING ANTENNA SIMULATIONS

This section focuses on the full integration of the conventional Vivaldi antenna with filtering structures, detailed in section II.

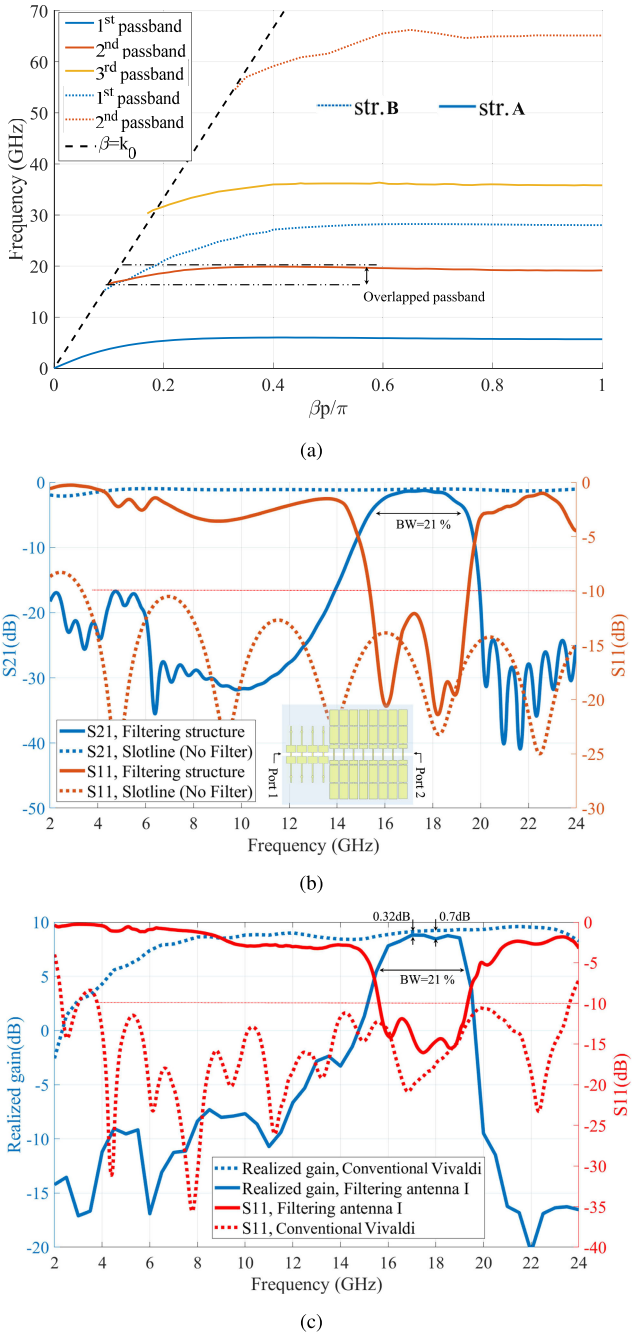

FIGURE 7. (a)The combined dispersion response of structures A and B with p1=p2=0.9mm, W=W2=0.8mm, L3=1.6mm, Ws=0.1mm, L5=1.2mm, s=0.4 mm. (b) The simulated S-parameters of a 2-port slotline (s=0.4mm) with the filtering structure, consisted of str. A and B on the middle layer, (solid line) and without filter (dotted line). (c) The simulated boresight realized gain and reflection coefficient (S11) of the filtering antenna I, depicted in Fig. 1(a), (solid lines) and conventional Vivaldi antenna (dotted lines).

Two filtennas, named filtering Vivaldi Antenna I and II, are designed to operate at 18GHz and 6.5GHz, respectively, as their center frequency.

A. FILTERING VIVALDI ANTENNA I

As a result of the findings in section II-B, the variation of the slotline's width, e.g. along the Vivaldi flare, has

a negligible impact on the filtering performance of the proposed structures. However, it does not imply that it can be disregarded. There are good reasons for subtle consideration due to the presence of a strip parallel to the electric field vector below the slotline. First, moving the filter farther along the flare results in a proportional increase in insertion loss, corresponding to the strip's length below the slotline. Second, their parasitic effects result in mismatch and unwanted scattering. Thus, it is recommended to place the structures at the beginning part of the antenna's flare, as depicted in Fig. 1(a). Here, the starting point of the filtering structures, e.g. the distance between the antenna feeding part and filtering structure, called Df, is tuned to achieve optimal in-band matching conditions.

The repetition count of the periodic structure's unit is another critical parameter. On one hand, it can improve the filtering roll-off rate and rejection; on the other hand, it prolongs the filtering structure resulting in going farther along the flare. Hence, a thoughtful trade-off according to the intended application is necessary. Here, we cascade structure B with structure A, beginning with structure B and then A, to obtain both improved impedance matching and wider stopband regions close to the feeding part. The combined dispersion response of structures A and B is depicted in Fig. 7(a), highlighting the wider stopband region of structure B (dotted lines) and the overlapped passband frequencies from 16-20GHz.

Fig. 7(b) shows the simulated S-parameters, utilizing the CST Studio Suit transient solver, for a 2-ports slotline, see Fig. 7(b) and 1(b), with and without the cascaded filtering structure on its middle layer. The filtering structure consists of 4 repetitions of structure B and 8 repetitions of structure A. The figure highlights the filtering performance with 21% fractional bandwidth (15.6-19.3GHz), wide out-of-band suppression (2-24 GHz), and low insertion loss (0.27dB). Increasing the repetition of structures B and A enhances the suppression level, e.g. 8 repetitions of structure B improve suppression below 6GHz. The slight difference in the passband response, from 16-20GHz in the dispersion diagram, see Fig. 7(a), to 15.6-19.3GHz, stems from the interactions between the physically cascaded structures B and A.

Fig. 7(c) depicts simulation results utilizing the CST Studio Suit transient solver for the fully integrated filtering antenna I, see Fig. 1(a). The filtenna incorporates the structures B and A. The figure highlights the filtering performance with 21% fractional bandwidth, low insertion loss of 0.32dB, and wide out-of-band suppression which effectively covers the entire frequency range of the conventional Vivaldi antenna (before the integration of structures B and A). The realized gain rapidly drops outside of the desired passband (15.6-19.3GHz). Typical values of $\geq$15dB suppression compared to the conventional Vivaldi are obtained. Only a narrow frequency range (12.5-14GHz) at the lower edge of the passband displays a gain suppression of $\geq$11dB. Observe that there is a good agreement between the dispersion diagram of the cascaded structures B and A, Fig. 7(a), the filtering structure response, Fig. 7(b), and the results of the filtering antenna I, Fig. 7(c). The agreement demonstrates that the design principles and procedures are applicable and can be used to accelerate the design process. The limited range (12.5-14GHz) with 11-15dB gain suppression may be attributed to the repetition count of the structure units and the mutual coupling among different parts of the filtenna geometry. It's worth noting that the steep roll-offs and wide out-of-band suppression, Fig. 7(c), are achieved by using only 4 repetitions of structure B and 8 repetitions of structure A.

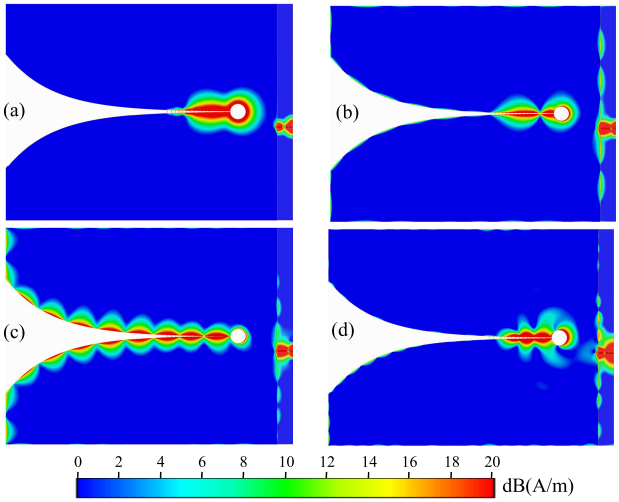

FIGURE 8. The simulated surface currents of the filtering antenna I, depicted in Fig. 1(a), at (a) 6GHz, (b) 12GHz, (c) 18GHz, (d) 24GHz.

When the frequency is below or above the intended passband, the wave can no longer propagate through the flare. This is validated by the simulated surface currents depicted in Fig. 8 at stopband frequencies of 6GHz, 12GHz, and 24GHz, along with a passband frequency of 18GHz. The figure shows that the filtering structures do not significantly affect the wave within the passband while effectively blocking waves outside of it.

B. FILTERING VIVALDI ANTENNA II

To practically demonstrate the capability of the band selectivity and operational bandwidth tuning of our approach, another filtering Vivaldi antenna, denoted as II, operating from 6.1-6.9GHz (12% fractional bandwidth) is introduced in Fig. 9(a). In the filtering antenna II, both the center frequency of the filter and its operational bandwidth are adjusted while the conventional Vivaldi antenna (base antenna) remains unchanged.

In this filtenna configuration, structures C, Fig. 1(c) and 6(b), and A are cascaded, with structure C placed first, then structure A. The center frequency and operational bandwidth of the filtering performance of structure A are tuned by employing the patch lengths and slight changes to both periodicity and width, Fig. 9(a). The combined dispersion response of the structures A (adjusted version) and C is depicted in Fig. 9(b), highlighting the overlapped

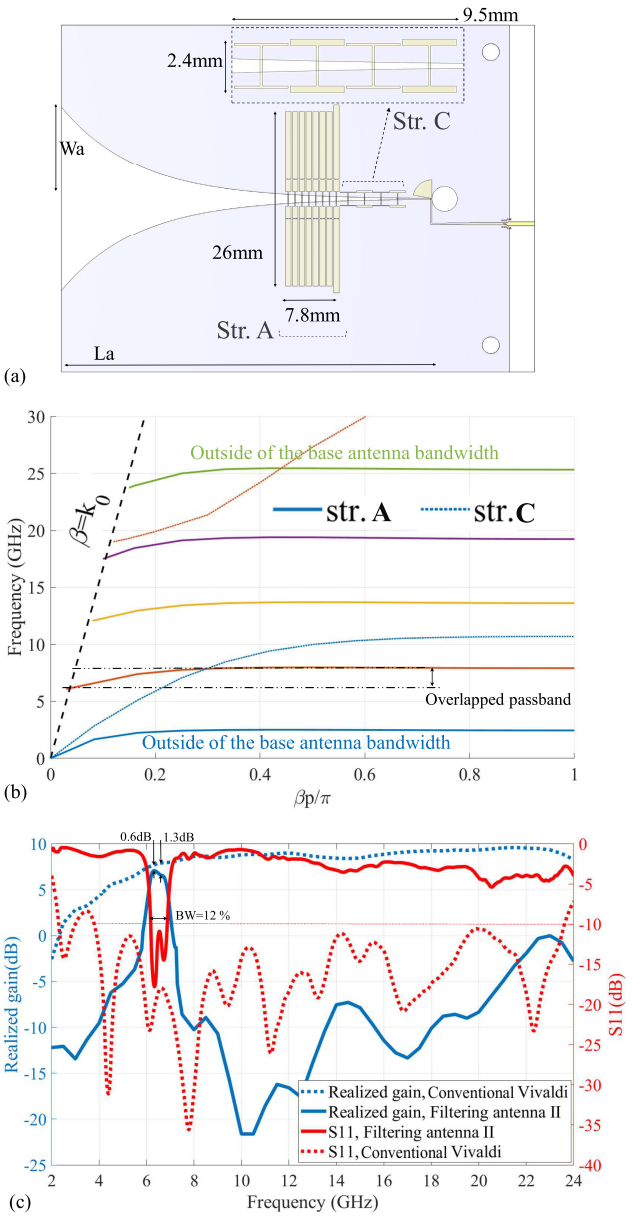

FIGURE 9. (a) Top view of the filtering Vivaldi antenna II operating from 6.1 to 6.9GHz,(b) The combined dispersion response of structures A and C with p1= 1mm, W=0.9mm, L3+L2=10.1mm, L1=1.75mm, s=0.4mm, p3=2.4mm, W3= 2.3mm, L6=0.3mm. (c) The simulated boresight realized gain and reflection coefficient (S11) of the filtering antenna II, depicted in Fig. 9(a), (solid lines) and conventional Vivaldi antenna (dotted lines).

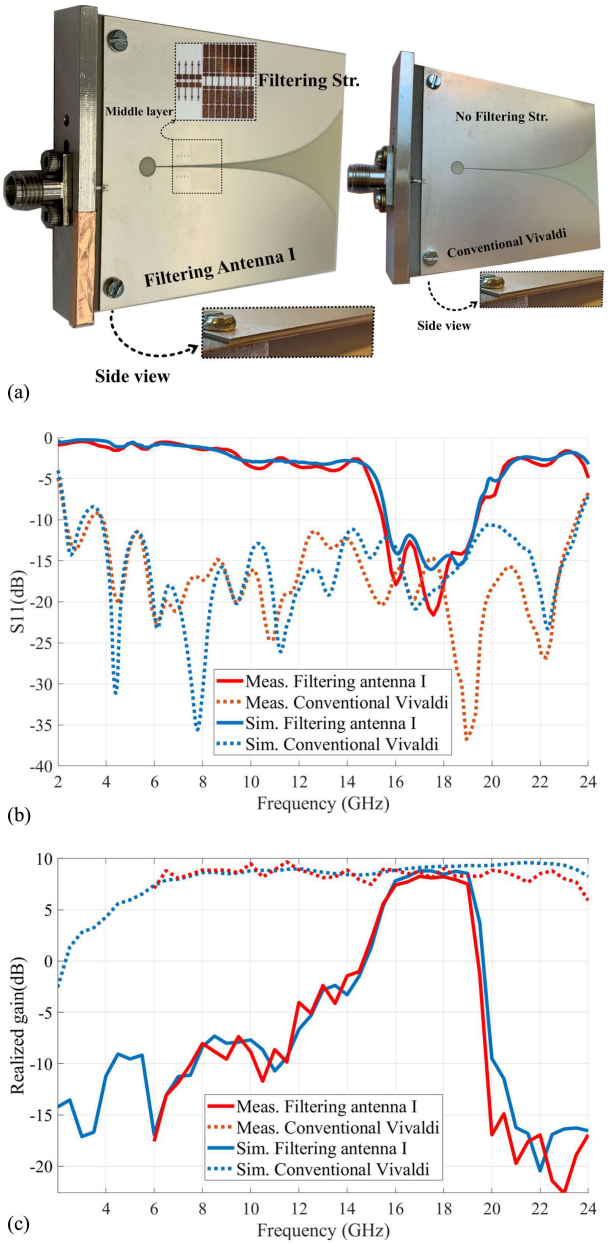

FIGURE 10. (a) The manufactured filtering antenna I with a zoomed view of its filtering structures, placed in the middle layer. Also shown is the manufactured conventional Vivaldi antenna (i.e. without filtering structures). The measured (red color) and simulated (blue color) (b) reflection coefficient (S11) and (c) boresight realized gain of the filtering antenna I and conventional Vivaldi antenna, depicted in Fig. 10(a).

passband. The conventional Vivaldi antenna functions well from 4GHz up to 24GHz, inherently filtering out lower and higher frequencies, such as those passbands exceeding 24GHz and lower than 2GHz in Fig. 9(b).

Fig. 9(c) represents simulation results achieved using CST Studio Suit transient solver for the filtering antenna II, Fig. 9(a), which incorporates both structures C and the adjusted version of A. The figure highlights the filtering performance with 12% fractional bandwidth, low insertion loss of 0.6dB, and wide out-of-band suppression which effectively covers the entire frequency range of the conventional Vivaldi antenna (before the integration of structures C and A). The insertion loss is slightly higher than the filtering antenna I due to larger filtering geometry leading to more conductive loss and larger periodicities causes going farther along the flare. The realized gain rapidly drops outside of the desired passband (6.1-6.9GHz), with a typical value of $\geq$15dB compared to the conventional Vivaldi. Only the frequency range from 21.5GHz to 24GHz, located at the end of the stopband, exhibits a gain suppression of between

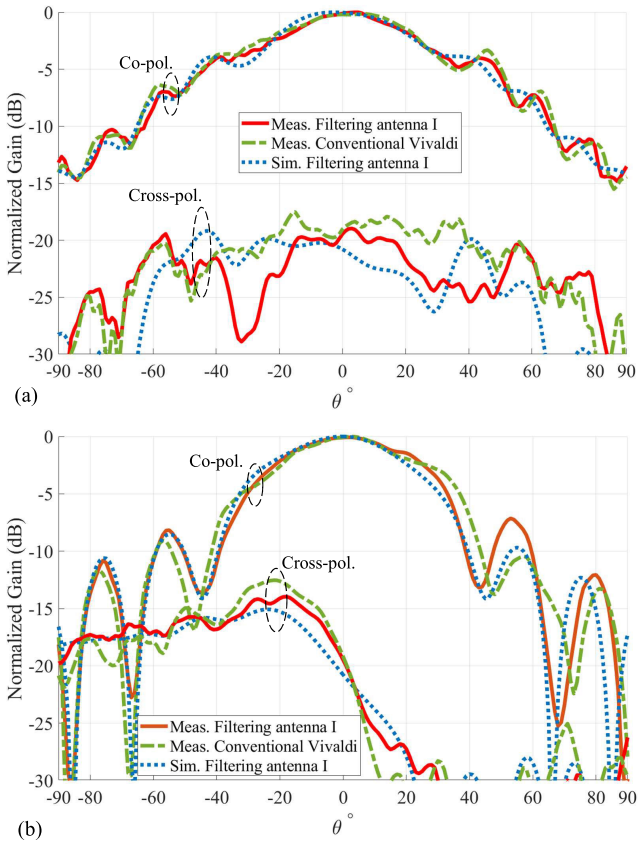

FIGURE 11. The normalized measured (solid line) and simulated (dotted line) radiation patterns of the filtering antenna I, depicted in Fig. 10(a), along with the measured radiation pattern of the conventional Vivaldi antenna (dash-dot line), depicted in Fig. 10(a), at 18GHz for the both (a) E-plane, (b) H-plane.

10-15dB, which might arise from internal coupling among filtenna parts and the repetition count of the structures A and C. A slight variation in the length of the units of the structures A and C, Fig. 9(a), is implemented to improve the behavior of the filtenna in the vicinity of the passband of S11.

It is worth noting that the proposed approach opens up the possibility of achieving an even wider out-of-band suppression by combining structures A, B, and C. The total filtering performance can be customized to match desired application requirements by carefully cascading these proposed structures, e.g. a wider out-of-band suppression frequency range.

IV. FABRICATION AND MEASUREMENT RESULTS

To experimentally validate the performance of the proposed approach, prototypes of the filtering antenna I and the conventional Vivaldi antenna are manufactured, depicted in Fig. 10(a). The filtering structures are positioned in the middle layer, highlighted in Fig. 10(a) using a dashed box for visibility. The conventional Vivaldi antenna with no integration (i.e. without filtering structures) is fabricated to provide a reference for realized gain and reflection coefficient comparisons.

TABLE 2. Comparison between proposed Filtering antenna structure and previous state-of-the-art solutions.

Ref.	[29]	[27]	[8]	[25]	This work
Radiating element (ABW[1])	Vivaldi (5:1)	Vivaldi ≈(4:1)	Vivaldi ≈(2:1)	Vivaldi (6:1)	Vivaldi (6:1)
Filtering method (function)	Corr. + finline (BPF)	SSPP str. (LPF[2])	coupled filter (BPF)	OCHWR +SCSIR[3] (Notch)	periodic str. (BPF or Notch)
Integration level	Highly	Highly	Highly	Fully	Fully
PB[4] selectivity (Oper. range) GHz	f_l:Comp.[5] f_h:Ctrl.[6] (1.2-3.5)	f_l:N/A[7] f_h:Ctrl. (15-30)	f_l:Ctrl. f_h:Ctrl. (25-44)	f_l:Ctrl. f_h:Ctrl. (2–12)	f_l:Ctrl. f_h:Ctrl. (4-24)
fractional FBW[8]	NB[9]-88%	NB-68%	19%	10-30%	NB-ABW
OOB G. supp.[10] level(dB) & range(GHz)	20 & 3-6 (10 in [.7-1])	14 & 27-30 (NR:>30)	NR[11]	14 & 4.9-6.6 (inband)	15 & 2-12, 19-24 (11 in [12.5-14])*
Insertion loss(dB)	NR	NR	0.5	NR	0.3*

[1]base antenna bandwidth, [2]LPF+lower aperture cutoff, [3]open and short-circuit T.L. resonator, [4]passband (f_l,f_h) GHz, [5]complicated, [6]controllable, [7]not applicable, [8]filtering bandwidth, [9]narrow band (≈ 10%), [10]out-of-band gain suppression, [11]not reported,*filtering antenna I,

The filtering antenna I and conventional antenna are measured in an anechoic chamber performing far-field measurements using a standard horn antenna as a probe and our antenna as DUT (device under test). To measure the value of realized gain and calibration, we utilize the classical gain substitution technique [40] with the same probe.

The measurement results in terms of S11 and realized gain are compared with simulation results and shown in Fig. 10(b) and 10(c), respectively. The good agreement of the reflection coefficient and realized gain across a wide frequency range (2-24GHz for S11 and 6-24GHz for realized gain) validates the filtering performance and our proposed approach. Our radiation pattern measurements covered a half-space $\theta \in [-90°, 90°]$ from 6GHz to 24GHz, limited in the lower band by the operating frequency range of our standard horn antenna in the anechoic chamber. Fig. 11 illustrates the measured and simulated radiation pattern of the filtering antenna prototypes at 18GHz, an in-band frequency, in both E-plane, Fig. 11(a), and H-plane, Fig. 11(b). The figure demonstrates that while the filtering structures effectively filter the unwanted out-of-band radiations, they have a negligible impact on the desired in-band radiation patterns and overall performance. The slight asymmetry and shifts in Fig. 11 come from a minor misalignment in the positioning in the anechoic chamber.

Table 2 compares the proposed filtering antenna structure with previously reported Vivaldi-based filtennas [8], [25], [27], [29]. The proposed multi-functional filtenna offers low insertion loss, wide out-of-band suppression (2-24GHz), adjustable fractional bandwidth (from approximately 10% up to the Vivaldi entire bandwidth), high band-selectivity with control over both higher and lower filter cut-off frequencies (f_l, f_h) across the wide operational Vivaldi range/bandwidth (6:1), and full integration while maintaining the original base antenna size. This performance represents a significant advancement compared to prior state-of-the-art designs.

V. CONCLUSION

This paper presents a novel approach for realizing fully integrated bandpass filtering Vivaldi antennas with high selectivity, adjustable operational bandwidth, and wide out-of-band suppression. Through cascading structurally similar configurations (structures A, B, and/or C), we have shown the capability to achieve versatile filtering performance. To validate our approach, the designed filtering Vivaldi antennas, called filtering antenna I and filtering antenna II, demonstrate different center frequencies of 18GHz and 6.5GHz, fractional bandwidth of 21% and 12%, low insertion loss of 0.32dB and 0.6dB, respectively. Furthermore, the realized filtennas have a wide out-of-band suppression of typically $\geq$15dB, effectively covering the entire frequency range of the conventional Vivaldi antenna (4-24GHz). The filtering antenna I prototype is manufactured and its measurement results, in terms of realized gain, reflection coefficient, and radiation patterns, demonstrate a good agreement with the simulation results. Experimental validation confirms the effectiveness of the proposed approach. The negligible impact on the in-band radiation patterns, controllable passband, tunable operational bandwidth, low insertion loss, and wide out-of-band suppression make the fully integrated approach suitable for a wide range of applications requiring efficient and adaptable frequency filtering, e.g. wireless communication, radar systems, and passive sensors.

REFERENCES

[1] J. L. Volakis, *Antenna Engineering Handbook*, vol. 1755. New York, NY, USA: McGraw-Hill, 2007.

[2] A. Emadeddin and B. L. G. Jonsson, "Wide scan, active *K*-band, direct-integrated phased array for efficient high-power Tx-generation," *IEEE Trans. Antennas Propag.*, vol. 71, no. 9, pp. 7579–7584, Sep. 2023, doi: 10.1109/TAP.2023.3281075. ,

[3] W.-C. Liao, R. Maaskant, T. Emanuelsson, V. Vassilev, O. Iupikov, and M. Ivashina, "A directly matched PA-integrated *K*-band antenna for efficient mm-wave high-power generation," *IEEE Antennas Wireless Propag. Lett.*, vol. 18, no. 11, pp. 2389–2393, Nov. 2019.

[4] C. X. Mao, Y. Zhang, X. Y. Zhang, P. Xiao, Y. Wang, and S. Gao, "Filtering antennas: Design methods and recent developments," *IEEE Microw. Mag.*, vol. 22, no. 11, pp. 52–63, Nov. 2021.

[5] A. K. Gangwar, M. S. Alam, V. Rajpoot, and A. K. Ojha, "Filtering antennas: A technical review," *Int. J. RF Microw. Comput.-Aided Eng.*, vol. 31, no. 10, Oct. 2021, Art. no. e22797.

[6] P. P. Shome, T. Khan, S. K. Koul, and Y. M. M. Antar, "Filtenna designs for radio-frequency front-end systems: A structural-oriented review," *IEEE Antennas Propag. Mag.*, vol. 63, no. 5, pp. 72–84, Oct. 2021.

[7] J. Yun, S. Trinh-Van, J.-Y. Park, Y. Yang, K.-Y. Lee, and K. C. Hwang, "Cavity-backed patch filtenna for harmonic suppression," *IEEE Access*, vol. 8, pp. 221580–221589, 2020.

[8] K. Yang, M. Hoang, X. Bao, P. McEvoy, and M. J. Ammann, "Dual-stub Ka-band Vivaldi antenna with integrated bandpass filter," *IET Microw., Antennas Propag.*, vol. 12, no. 5, pp. 668–671, Apr. 2018.

[9] W. T. Li, Y. Q. Hei, H. Subbaraman, X. W. Shi, and R. T. Chen, "Novel printed filtenna with dual notches and good out-of-band characteristics for UWB-MIMO applications," *IEEE Microw. Wireless Compon. Lett.*, vol. 26, no. 10, pp. 765–767, Oct. 2016.

[10] G.-H. Sun, S.-W. Wong, L. Zhu, and Q.-X. Chu, "A compact printed filtering antenna with good suppression of upper harmonic band," *IEEE Antennas Wireless Propag. Lett.*, vol. 15, pp. 1349–1352, 2016.

[11] C.-T. Chuang and S.-J. Chung, "Synthesis and design of a new printed filtering antenna," *IEEE Trans. Antennas Propag.*, vol. 59, no. 3, pp. 1036–1042, Mar. 2011.

[12] Y.-X. Huang, Y.-X. Yan, W. Yu, W. Qin, and J.-X. Chen, "Integration design of millimeter-wave bidirectional endfire filtenna array fed by SIW filtering power divider," *IEEE Antennas Wireless Propag. Lett.*, vol. 21, no. 7, pp. 1457–1461, Jul. 2022.

[13] D. Kumar Choudhary and R. Kumar Chaudhary, "Compact filtering antenna using asymmetric CPW-fed based CRLH structure," *AEU-Int. J. Electron. Commun.*, vol. 126, Nov. 2020, Art. no. 153462.

[14] A. Kumar and S. Imaculate Rosaline, "Hybrid half-mode SIW cavity-backed diplex antenna for on-body transceiver applications," *Appl. Phys. A, Solids Surf.*, vol. 127, no. 11, pp. 1–7, Nov. 2021.

[15] A. Kumar and S. Raghavan, "Planar cavity-backed self-diplexing antenna using two-layered structure," *Prog. Electromagn. Res. Lett.*, vol. 76, pp. 91–96, 2018.

[16] H. Qi and H. Liu, "Single-ended band-notched Vivaldi antenna with common mode suppression and low cross polarization," *IEEE Antennas Wireless Propag. Lett.*, vol. 20, no. 10, pp. 1983–1987, Oct. 2021.

[17] C. Chen, "A compact wideband endfire filtering antenna inspired by a uniplanar microstrip antenna," *IEEE Antennas Wireless Propag. Lett.*, vol. 21, no. 4, pp. 853–857, Apr. 2022.

[18] S. J. Yang, Y. F. Cao, Y. M. Pan, Y. Wu, H. Hu, and X. Y. Zhang, "Balun-fed dual-polarized broadband filtering antenna without extra filtering structure," *IEEE Antennas Wireless Propag. Lett.*, vol. 19, no. 4, pp. 656–660, Apr. 2020.

[19] C. F. Ding, X. Y. Zhang, and M. Yu, "Simple dual-polarized filtering antenna with enhanced bandwidth for base station applications," *IEEE Trans. Antennas Propag.*, vol. 68, no. 6, pp. 4354–4361, Jun. 2020.

[20] X. Y. Zhang, W. Duan, and Y.-M. Pan, "High-gain filtering patch antenna without extra circuit," *IEEE Trans. Antennas Propag.*, vol. 63, no. 12, pp. 5883–5888, Dec. 2015.

[21] J. Kukreja, D. K. Choudhary, and R. K. Chaudhary, "A short-ended compact metastructure antenna with interdigital capacitor and U-shaped strip," *Wireless Pers. Commun.*, vol. 108, no. 4, pp. 2149–2158, Oct. 2019.

[22] M. R. Hamid, P. Gardner, P. S. Hall, and F. Ghanem, "Vivaldi antenna with integrated switchable band pass resonator," *IEEE Trans. Antennas Propag.*, vol. 59, no. 11, pp. 4008–4015, Nov. 2011.

[23] C. Wang, X. Wang, H. Liu, Z. Chen, and Z. Han, "Substrate integrated waveguide filtenna with two controllable radiation nulls," *IEEE Access*, vol. 8, pp. 120019–120024, 2020.

[24] W. Yang, S. Chen, Q. Xue, W. Che, G. Shen, and W. Feng, "Novel filtering method based on metasurface antenna and its application for wideband high-gain filtering antenna with low profile," *IEEE Trans. Antennas Propag.*, vol. 67, no. 3, pp. 1535–1544, Mar. 2019.

[25] Y. Xu, J. Wang, L. Ge, X. Wang, and W. Wu, "Design of a notched-band Vivaldi antenna with high selectivity," *IEEE Antennas Wireless Propag. Lett.*, vol. 17, no. 1, pp. 62–65, Jan. 2018.

[26] C.-X. Mao, S. Gao, Y. Wang, and Z. Cheng, "Filtering antenna with two-octave harmonic suppression," *IEEE Antennas Wireless Propag. Lett.*, vol. 16, pp. 1361–1364, 2017.

[27] H. Qi and H. Liu, "Wideband high-gain filtering Vivaldi antenna design based on MS and herringbone SSPP structure," *IEEE Antennas Wireless Propag. Lett.*, vol. 22, no. 8, pp. 1798–1802, Aug. 2023.

[28] H. Liu, Z. Wang, Q. Zhang, H. Ma, B. Ren, and P. Wen, "Design wideband differential bandpass filter using slotline surface plasmon polaritons," *IEEE Access*, vol. 7, pp. 44212–44218, 2019.

[29] M. Kuosmanen, J. Holopainen, J. Ala-Laurinaho, T. Kiuru, and V. Viikari, "Filtering antenna array based on corrugated Vivaldi elements," *IEEE Trans. Antennas Propag.*, vol. 71, no. 8, pp. 6546–6557, Aug. 2023.

[30] S. Lizhong and F. Qingyuan, "Design and measurement of a kind of dual polarized Vivaldi antenna," in *Proc. Cross Strait Quad-Regional Radio Sci. Wireless Technol. Conf.*, vol. 1, Jul. 2011, pp. 494–497.

[31] A. Bhattacharjee, A. Bhawal, A. Karmakar, A. Saha, and D. Bhattacharya, "Vivaldi antennas: A historical review and current state of art," *Int. J. Microw. Wireless Technol.*, vol. 13, no. 8, pp. 833–850, Oct. 2021.

[32] T. Maleszka and G. Jaworski, "Broadband stripline to microstrip transition with constant impedance field matching section for applications in multilayer planar technologies," in *Proc. 18-th Int. Conf. Microw., Radar Wireless Commun.*, Jun. 2010, pp. 1–4.

[33] C. Kolitsidas, "The strongly coupled asymmetric dipole array (SCADA) with an E-plane edge termination," Ph.D dissertation, KTH Roy. Inst. Technol., Stockholm, Sweden, 2017. [Online]. Available: https://urn.kb.se/resolve?urn=urn

[34] M. Moosazadeh, S. Kharkovsky, J. T. Case, and B. Samali, "Antipodal Vivaldi antenna with improved radiation characteristics for civil engineering applications," *IET Microw., Antennas Propag.*, vol. 11, no. 6, pp. 796–803, May 2017.
[35] J. T. Logan, R. W. Kindt, and M. N. Vouvakis, "Low cross-polarization Vivaldi arrays," *IEEE Trans. Antennas Propag.*, vol. 66, no. 4, pp. 1827–1837, Apr. 2018.
[36] M. Amiri, F. Tofigh, A. Ghafoorzadeh-Yazdi, and M. Abolhasan, "Exponential antipodal Vivaldi antenna with exponential dielectric lens," *IEEE Antennas Wireless Propag. Lett.*, vol. 16, pp. 1792–1795, 2017.
[37] X. Li, D. W. Pang, H. L. Wang, Y. Zhang, and G. Lv, "Dielectric sheets covered broadband Vivaldi antenna for gain enhancement," *Prog. Electromagn. Res. C*, vol. 77, pp. 69–80, 2017.
[38] L. Sang, X. Li, T. Chen, and G. Lv, "Analysis and design of tapered slot antenna with high gain for ultra-wideband based on optimisation of the metamaterial unit layout," *IET Microw., Antennas Propag.*, vol. 11, no. 6, pp. 907–914, May 2017.
[39] A. F. Harvey, "Periodic and guiding structures at microwave frequencies," *IEEE Trans. Microw. Theory Techn.*, vol. MTT-8, no. 1, pp. 30–61, Jan. 1960.
[40] G. Evans, *Antenna Measurement Techniques* (Antennas and Propagation Library). Norwood, MA, USA: Artech House, 1990.

AHMAD EMADEDDIN received the B.S. and M.S. degrees in electrical engineering from Shahed University, Tehran, Iran, in 2010 and 2012, respectively. He is currently pursuing the Ph.D. degree with the School of Electrical Engineering and Computer Science (EECS), KTH Royal Institute of Technology, Stockholm, Sweden.

He was an RF/Antenna Designer and a Researcher with IPMS Company, Tehran, between 2010 and 2018. His current research interests include active integrated phased array antenna, active devices, array clustering, filtenna, metasurfaces, and multi-beam antenna systems.

B. L. G. JONSSON received the M.Sc. degree in engineering physics from Ume University, in 1995, and the Ph.D. degree in engineering (electromagnetic theory) from the KTH Royal Institute of Technology, Stockholm, Sweden, in 2001. He was a Postdoctoral Fellow with the University of Toronto, Canada, and a Wissenschaftlicher Mitarbeiter (Postdoctoral) with ETH Zürich, Switzerland. He joined the Electromagnetic Engineering Laboratory, KTH, in 2006, where he became a Docent in electromagnetic theory, in 2006. He is currently a Professor in electromagnetic fields and the Deputy Director of Third Cycle Education with EECS/KTH. His research interests include electromagnetic theory, antennas, arrays, scattering theory, effective models, physical bounds, and nonlinear dynamics.